Journal of Alloys and Compounds 505 (2010) 352–356

Contents lists available at ScienceDirect

Journal of Alloys and Compounds

journal homepage: www.elsevier.com/locate/jallcom

Synthesis and characteristic of carbon-encapsulated ferronickel nanoparticles by detonation decomposition of doping with nitrate explosive precursors

Luo Ning [a,*], Li Xiaojie [a], Sun Yuling [b], Wang Xiaohong [a]

[a] State Key Laboratory of Structural Analysis for Industrial Equipment, Dalian University of Technology, Dalian 116024, China
[b] Artillery Academy of PLA, Hefei 230031, China

ARTICLE INFO

Article history:
Received 11 January 2010
Received in revised form 10 May 2010
Accepted 14 May 2010
Available online 18 June 2010

Keywords:
Composite nanoparticles
Nanostructure
Detonation synthesis
Transmission electron microscopy
Magnetic properties

ABSTRACT

Synthesizing carbon-encapsulated ferronickel nanoparticles was developed by a detonation method. The composite precursors were ignited in the nitrogen in closed explosion vessel. These composite nanoparticles were characterized with transmission electron microscope, energy-dispersive X-ray spectrometer, X-ray diffraction, X-ray fluorescence, Raman spectroscopy and magnetic measurement. Results indicated that carbon-encapsulated ferronickel nanoparticles with diameters ranging from 10 to 50 nm were produced and the composite nanoparticles were with a core–shell structure. The composite nanoparticles were synthesized with the yield about 10–15% one time.

1. Introduction

The graphite carbon shell protects the metallic core against oxidization and further agglomeration to form bigger crystallites. Saito [1,2] revealed that rare-earth metals with low vapor pressure (Sc, Y, La, Ce, Pr, etc.) were encapsulated in the form of carbides, while the volatile Sm, Eu and Yb metals showed no evidence of being wrapped in graphitic carbon by using electric arc discharge method. So far, a number of strategies for preparing CEMNPs have been developed, including modified arc discharge [3,4], chemical vapor deposition (CVD) [5], high-temperature heat treatment [6], ion-beam sputtering methods [7] and heat-induced explosion [8], etc. Specifically, Fe, Ni and Co have received the most interest due to their ferromagnetic properties and their unique catalyzing ability [9–11].

High level energy consumption and intricate uses of various facilities of the methods hinder the preparation of carbon-encapsulated metal nanocrystals in high yield. Accordingly, using detonation method [12–14] to synthesizing carbon-encapsulated metal nanoparticles (CEMNPs) is being an effective way and subsequent characterization of the properties of these nanoparticles are currently being actively investigated. Currently, only a few studies have dealt with carbon-encapsulated ferronickel alloy nanomaterials. Therefore, studies investigating a more efficient technique to encapsulate metal nanoparticles with a core–shell structure are required.

In this work, a simple and efficient technique for preparing carbon-encapsulated ferronickel composite nanoparticles was described. The detonation of composite explosive precursors not only produced powerful shock waves but also provided elemental building blocks and an unique high-pressure and high-temperature physical environment for the construction of various nanostructures [15]. Due to their potential application for magnetic materials, biological materials and catalyzers, graphite-encapsulated alloy composite nanoparticles were synthesized by detonation decomposition of explosive precursors doping with a soluble nitrate (metal source) and acetone/cyclonite (carbon source).

2. Experimental

The detonation synthesis of nanoparticles were performed in an explosion vessel as described in the previous work [16,17]. To synthesize ferronickel@C nanoparticles, iron nitrate and nickel nitrate ($Fe(NO_3)_3{\cdot}9H_2O$, $Ni(NO_3)_2{\cdot}6H_2O$) were selected as metal source materials for explosive precursors, together with carbon source materials such as pentaerythritol tetranitrate/cyclonite. The metallic sources were mixed with a given mole ratio of 2:1 and 1:1. All the chemical reagents used in this study were analytical grade. In a typical experimental procedure, the as-prepared composite precursors were placed into the closed explosion vessel about 0.4 m^3 capacity filling with nitrogen gas. After detonation reaction, the black powders were scraped from the inner explosion vessel. The powders were washed with absolute ethyl alcohol solution and then dried up in air. The composite nanoparticles were synthesized with the yield about 10–15% one time, that is, it takes one kilograms of precursors to make 100–150 gram of the composite nanoparticles.

Transmission electron microscope (TEM, operating at 200 kV) was used to reveal the morphology and microstructure of the nanoparticles. The TEM samples were

* Corresponding author. Tel.: +86 18940935017; fax: +86 041184708307.
E-mail addresses: roling8080@163.com (N. Luo), dymat@163.com (X.J. Li).

0925-8388/$ – see front matter © 2010 Elsevier B.V. All rights reserved.
doi:10.1016/j.jallcom.2010.05.181

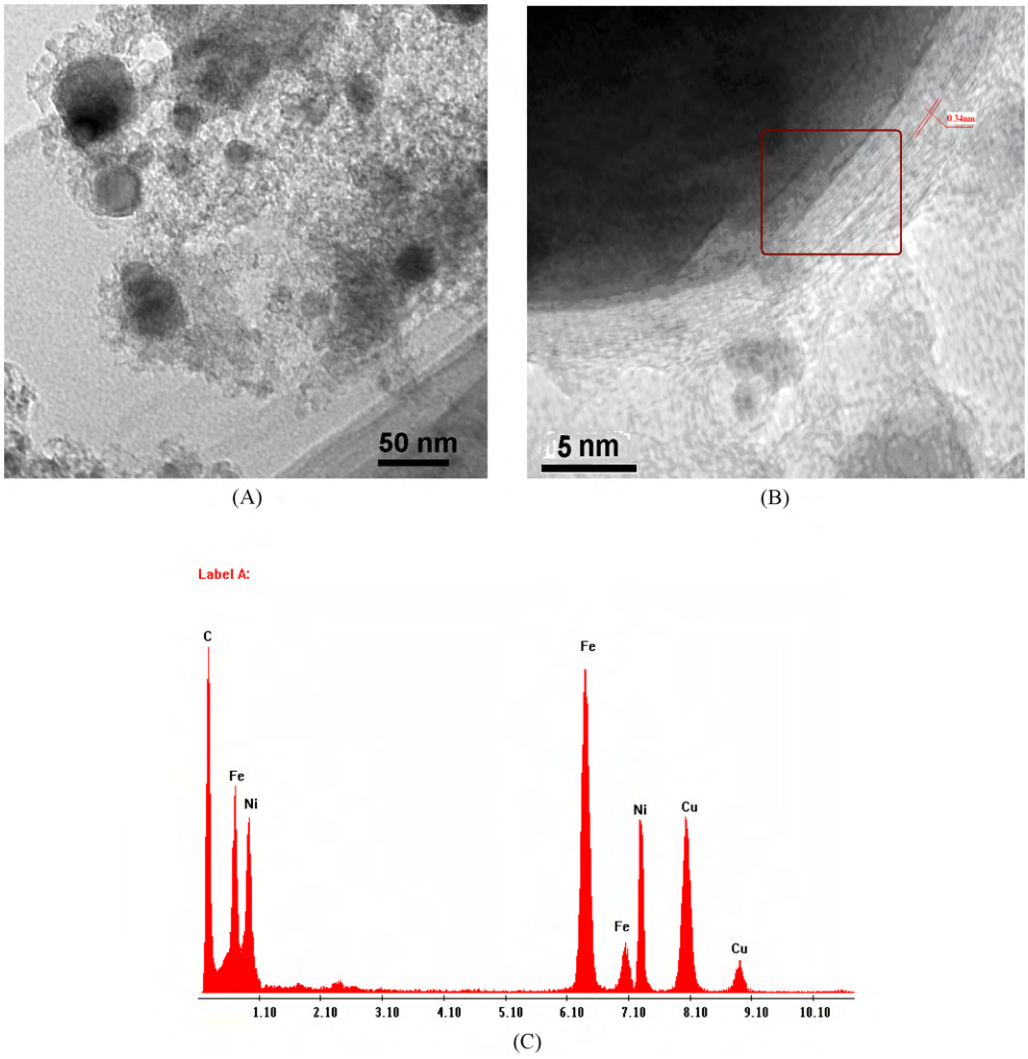

Fig. 1. (A and B) TEM images of carbon-encapsulated ferronickel nanoparticles with different magnification from sample no. 1; (C) EDX spectrum of single carbon-encapsulated ferronickel nanoparticle on selected field.

prepared by dispersing the nanoparticles in absolute ethyl alcohol with ultrasonic field for three minutes and then scooped up with a holy amorphous carbon film, drying a drop of the suspension on a copper grid. The chemical composition of composite nanoparticles in the samples were analyzed by the equipped energy-dispersive X-ray spectrometer (EDX). X-ray diffraction (XRD, using Cu Ka radiation) was employed to identify the phases and the crystal structures. X-ray fluorescence (XRF, series-1800X) was used to give us some basic components of detonation products concerning the elemental distributions based on the qualitative analysis. Raman spectroscopy (Renishaw Micro-Raman 2000, 632.8 nm He-Ne laser excitation) was used to investigate the base components of carbon shell layers. The magnetic properties of the nanoparticles at room temperature were measured by a vibrating sample magnetometer (VSM) operated with applied magnetic fields up to 2 T. The saturation magnetization (M_s), remanence magnetization (M_r) and coercivity field (H_c) values were obtained from the hysteresis loops.

3. Results and discussion

3.1. TEM analysis

Some composite nanoparticles are shown in Figs. 1A and 2A with the size of about 10–50 nm. The morphology of a single-particle from the some particles are shown in Figs. 1B and 2B and the selected red area corresponding EDX patterns for ferronickel@C are illustrated in Figs. 1C and 2C. It can be seen that ferronickel nanoclusters are uniformly embedded in a graphite carbon matrix, forming spherical nanoparticles with ferronickel solid phase.

TEM analysis reveals that all of the spheroidal particles have a core–shell structure with a big ferronickel core and graphite carbon shell. The carbon layers tightly encapsulate the black nanocrystal core (Figs. 1B and 2B), and no obvious voids could be observed between the core and the shell. The shells are uniform in thickness about 5–7 nm (Fig. 1B) usually consisted of 13–20 layers, or about 3–5 nm (Fig. 2B) which are of 10–15 layers. The spacing of the lattice fringes is about 0.34 nm, which is close to the distance between graphite layer.

The EDX image of the selected red area for the nanoparticle was analyzed as shown in Figs. 1C and 2C. The peaks around 8.00 and 9.00 keV corresponded to Cu Ka and Cu Kβ, which resulted from the copper of the copper grid used to support the nanoparticles. The EDX results showed that the solid phase consisted of iron/nickel elements corresponding to peaks around 1.00, 6.50 and 7.50 and carbon. From Figs. 1C and 2C, the peak intensity of iron/nickel are different between each other, whose the intensity ratio of iron/nickel were about 2:1 and 1:1 corresponding to the mole ratio of iron/nickel ions in explosive precursors.

3.2. XRD analysis

The crystallization of the nanoparticles were apparent by XRD (shown in Fig. 3). The main peaks appearing at $2\theta = 43.60^\circ$, 50.82°

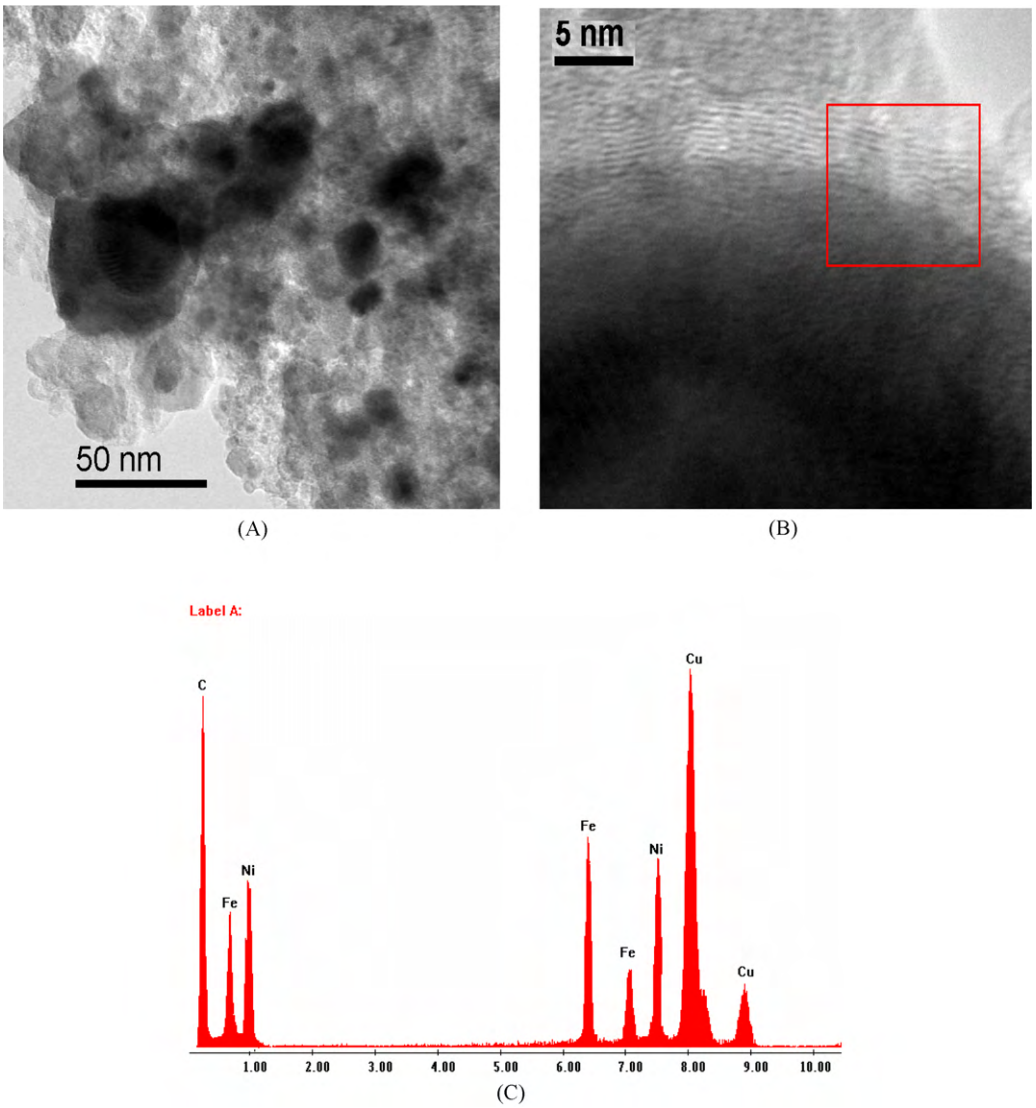

Fig. 2. (A and B) TEM images of carbon-encapsulated ferronickel nanoparticles with different magnification from sample no. 2; (C) EDX spectrum of single carbon-encapsulated ferronickel nanoparticle on selected field.

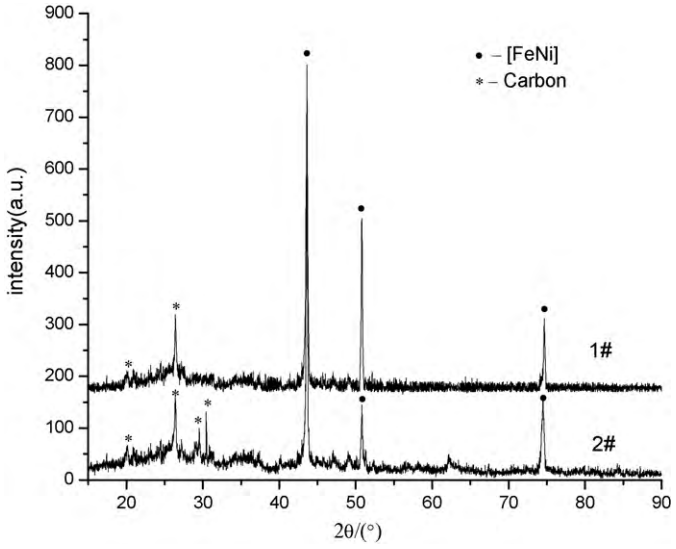

Fig. 3. XRD pattern of detonation products.

and 74.68° can be ascribed to the diffraction of the (1 1 1), (2 0 0) and (2 2 0) planes of alpha-ferronickel crystal (JCPDS No. 47-1405) from the sample no. 1. According to the sample no. 2, the main peaks appearing at $2\theta = 44.58°$, 50.80° and 74.50° can match with the diffraction of the (1 1 1), (2 0 0) and (2 2 0) planes of gamma-ferronickel crystal (JCPDS no. 47-1417), suggesting that the present composite nanoparticles are mainly composed of ferronickel alloy phase. The diffraction peak at about 26.4° can be assigned to the (0 0 2) plane of a hexagonal graphite structure (JCPDS no. 41-1487) with an interlayer spacing of about 0.34 nm. The fact that the narrower peak suggests a relatively well degree of graphite crystallization from the sample no. 1, meanwhile the sample no. 2 as shown in Fig. 3, there are still a certain amount of amorphous carbon in it.

From Fig. 3 and Table 1, the as-prepared composite nanoparticles are mainly composed of alpha- or gamma-ferronickel and graphite carbon. The crystal lattice distance of single-phase fcc-region of the ferronickel phase is about 0.2061 and 0.2074 nm which are from the XRD data. And with full width at half maximum, the mean diameter of nanoparticles are about 32.8 and 27.8 nm by the Scherrer formula. The mean particle sizes estimated from XRD data are consistent with the results of TEM observation.

Table 1
The related parameters of crystal lattice structure of detonation products.

Sample no.	2θ/°			FWHM/°	D/nm	[FeNi]
1#	43.60	50.82	74.68	0.243	32.8	Alpha-type
2#	44.58	50.80	74.50	0.287	27.8	Gamma-type

Note: *D*—the mean diameters of nanoparticles by Scherrer formula.

Table 2
The main element contents of the composite explosives by XRF.

Sample no.	C Ka	Fe Ka	Ni Ka	Others Ka
1#	43.6580%	34.9865%	17.6628%	4.6927%
2#	45.8046%	24.6868%	23.5954%	5.9132%

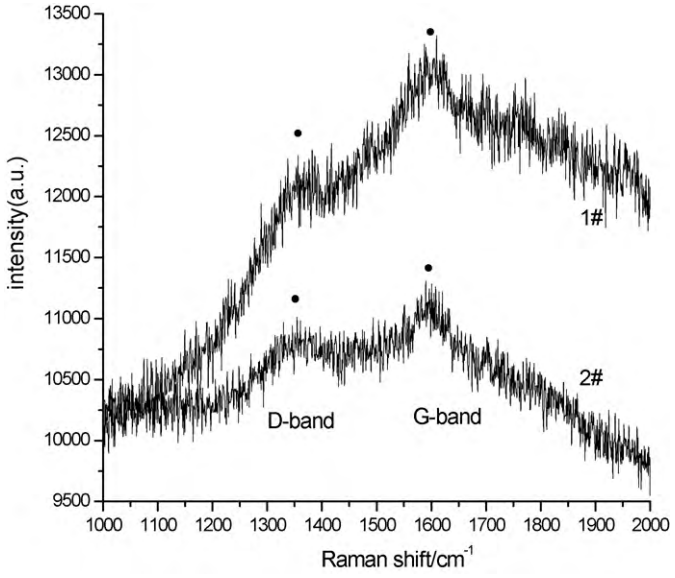

Fig. 4. Raman spectra of detonation products.

3.3. XRF and Raman analysis

In order to further quantitative investigations of detonation products, the XRF were carried out to characterize the as-obtained detonation powder. The results showed the basic elemental components of detonation products (such as Table 2).

The detonation products mainly consist of three kinds of elements such as carbon, iron and nickel, which amount to about 95%. The others elements are much relatively smaller only about 5%, which come from the non-reaction completely products or the ingredients of explosive precursors. From Table 2, the mole ratio of Fe^{3+} to Ni^{2+} is about 2:1 and 1:1, which equal to the metallic sources of explosive precursors. So detonation method may be provided an effective method for carbon-encapsulated alloy nanoparticles, which are under research.

It's well-known that the intensity of D- and G-peaks can be used to estimate the size of small crystalline graphite or to represent the disorder degree of graphite, comparing to the two typical carbon peak distribution of 1360 cm^{-1} amorphous carbon and 1585 cm^{-1} graphitic carbon [16]. The surface of detonation products were analysized by Raman spectroscopy to detect the species covering the surface. Clearly observed from Fig. 4, the Raman spectra of as-obtained detonation products revealed the distribution of amorphous carbon and graphitic carbon, which D-band at 1336.84 cm^{-1} and G-band at 1588.1 cm^{-1} (sample no. 1) and that of D-band 1335.90 cm^{-1} and G-band 1587.76 cm^{-1} (sample no. 2). Fig. 4 displays that the intensity of the amorphous carbon was lower than that of the graphitic and the intensity of graphitic carbon from sample no. 1 is higher than that from sample no. 2. In other words, there mainly are in the form of graphite within the carbon layers and carbon coating layers of sample no. 1 have a relatively well degree of graphite crystallization in according with the results of XRD analysis.

Table 3
The magnetic parameters database of detonation products.

Sample no.	M_r/emu/g	M_s/emu/g	H_c/Oe	M_r/M_s
1#	1.07	28.98	56	0.036
2#	0.71	35.56	43	0.020

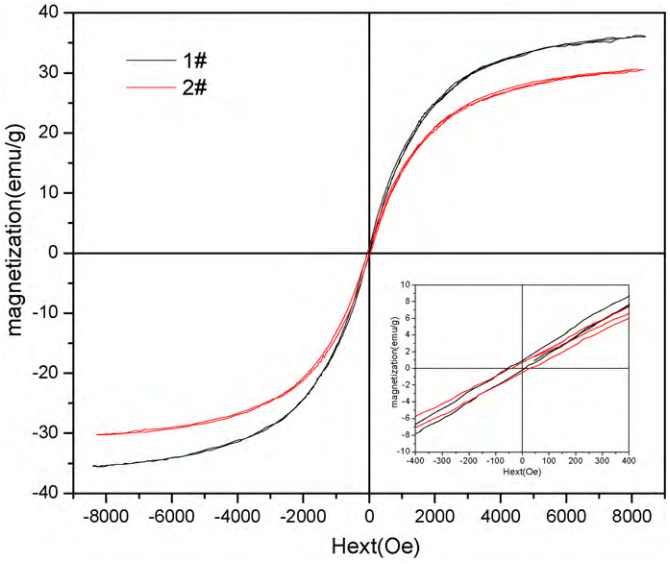

Fig. 5. The hysteresis loop of carbon-encapsulated ferronickel nanoparticles.

3.4. Magnetism analysis

For the magnetic nanoparticles, due to the larger surface and the change of the shape of the material, the smaller particles could have a larger surface anisotropy and a larger shape anisotropy, they should have a much smaller magnetocrystalline anisotropy due to the less contributions of the less magnetic atoms. Generally, the magnetocrystalline anisotropy of the nanoparticles increases with increasing the size of the magnetic nanoparticles. Thus the magnetic particles with a smaller size have a smaller coercive force [18]. Furthermore, the decrease of the size of the particles may result in the occurrence of the super-paramagnetism in part of the nanoparticles with size below the critical size.

To characterize the magnetic property of as-prepared products, the magnetic measurement was carried out at room temperature by VSM. For the magnetic nanoparticles, the magnetic properties, especially the saturation magnetization M_s and coercive force H_c, are dependent upon chemical composition and particle size. The VSM magnetic properties of the as-prepared ferronickel@C, the magnetic curves measured at room temperature are shown in Table 3 and Fig. 5. The results show a superparamagnetic response for ferronickel@C as suggested from the data on H_c, M_r, M_s and M_r/M_s. From the inserted image, the hysteresis loops of as-obtained products are partial enlarged view and fine narrower when the normal magnetic intensity is at zero point.

4. Conclusion

Carbon-encapsulated ferronickel nanoparticles have been synthesized successfully by a detonation method. The nanoparticles

have a diameter ranging from 10 to 50 nm with a perfect core–shell structure and the shell were mainly composed of graphite layers. The XRD, XRF and Raman measurements revealed that the cores of the as-prepared carbon nanocapsules were alpha-ferronickel and gamma-ferronickel and the coating layers of composite nanoparticles were graphite carbon and a certain amount of amorphous carbon. The magnetic measurements showed that the as-prepared nanocomposites had good super-paramagnetism. Based on above experimental results, using the strategy mentioned above, a simple route to synthesize carbon-encapsulated ferronickel nanoparticles with the yield about 10–15% can be prepared with one detonation reaction process. Due to the simplicity of the apparatus and good productivity of the present technique, it may offer a very attractive way for the production of ferronickel@C on large scale.

Acknowledgements

This research was financially supported by the Natural Science Foundation of China (Nos. 10602013, 10872044, 10902023) and the National Science foundation of Liaoning province of China (No. 2008161).

References

[1] Y. Saito, M. Okuda, T. Yoshikawa, J. Phys. Chem. 98 (1994) 6696.
[2] Y. Saito, Carbon 33 (1995) 979.
[3] B.S. Xu, J.J. Guo, X.M. Wang, X.G. Liu, I. Hideki, Carbon 40 (2006) 2631.
[4] G. Xing, S.L. Jia, Z.Q. Shi, New Carbon Mater. 22 (2007) 337.
[5] C.N. He, X.W. Du, J. Ding, C.S. Shi, J.J. Li, N.Q. Zhao, L. Cui, Carbon 44 (2006) 2330.
[6] J.P. Huo, H.H. Song, X.H. Chen, S.Q. Zhao, C.M. Xu, Mater. Chem. Phys. 101 (2007) 221.
[7] J. Nishijo, C. Okabe, J. Bushiri, K. Kosugi, N. Nishi, H. Sawa, Eur. Phys. J. D. 34 (2005) 219.
[8] Y. Lu, Z.P. Zhu, Z.Y. Liu, Carbon 43 (2005) 369.
[9] M. Bystrzejewski, A. Huczko, H. Lange, P. Baranowski, G. Cota-Sanchez, G. Soucy, Mater. Chem. Phys. 18 (2007) 145608.
[10] A. Ebara, K. Kuramochi, T. Yamazaki, I. Hashimoto, K. Watanabe, Carbon 45 (2007) 898.
[11] J.N. Wang, L. Zhang, F. Yu, Z.M. Sheng, J. Phys. Chem. B 111 (2007) 2119.
[12] J.J. Liu, H.L. He, X.G. Jin, Mater. Res. Bull. 36 (2001) 2357.
[13] A.A. El-Gendy, E.M.M. Ibrahim, V.O. Khavrus, Y. Krupskay, Carbon 47 (2009) 2821.
[14] N. Luo, X.J. Li, H.H. Yan, X.H. Wang, L.H. Wang, J. Chin, High Press. Phys. 23 (2009) 415.
[15] Z.P. Zhu, Mod. Phys. Lett. B 17 (2003) 1477.
[16] N. Luo, X.J. Li, X.H. Wang, H.H. Yan, F. Mo, W. Sun, Comp. Sci. Technol. 69 (2009) 2554.
[17] G.L. Sun, X.J. Li, Y.J. Zhang, X.H. Wang, D.A. Jiang, F. Mo, J. Alloys Compd. 473 (2009) 212.
[18] Z.H. Wang, C.J. Choi, B.K. Kim, J.C. Kim, Z.D. Zhang, Carbon 41 (2003) 1751.